Kinematics, topology and significance of dune-related macroturbulence: some observations from the laboratory and field

JIM BEST

Earth and Biosphere Institute, School of Earth and Environment, University of Leeds, Leeds, West Yorkshire LS2 9JT, UK (Email: j.best@earth.leeds.ac.uk)

ABSTRACT

Macroturbulence, which may advect through the entire water depth, dominates the flow field associated with alluvial sand dunes and has long been regarded as the principal mechanism for suspending bedload sediment over dunes. The origin of this macroturbulence has been linked to shear layer development in the dune lee, often associated with flow separation, and the form of these coherent flow structures has been noted as 'boils' that erupt onto the water surface. Although past work has quantified the mean and turbulent flow characteristics of flow over dunes using at-a-point measurements, these studies have not been able to trace the *evolution* of such macroturbulent events over a dune-covered bed. Additionally, the topology of the dune-related macroturbulence has not been explained in relation to the structure of the developing surface boils. This paper tackles both of these issues using a twofold approach: (i) use of whole flow field quantification using particle imaging velocimetry (PIV) over a series of fixed laboratory dunes; (ii) observations of the water surface over large sand dunes in the Jamuna River, Bangladesh.

Particle imaging velocimetry results are in good agreement with past work detailing the mean flow field over sand dunes. The PIV images over the lee and stoss sides of an experimental dune, and observation of the water surface above natural dunes, reveal four key dynamic attributes to flow.

1 The shear layer and separation zone associated with dunes are spatially and temporally dynamic, and 'flapping' of the shear layer may be modulated by turbulent coherent flow structures generated upstream.

2 Reynolds stresses in the lee side are dominated by the free shear layer associated with the separation zone.

3 Ejections of low downstream momentum fluid away from the bed dominate the instantaneous flow field over the crestal regions of the dune. These ejections, in turn, however, create return flows towards the bed both in front of, and behind, the ejection. The highest instantaneous Reynolds stresses are associated with these ejections and inrushes.

4 'Boils' on the water surface over a natural dune field often consist, firstly, of a central upwelling that has a spanwise axis of rotation and, secondly, later secondary vortices that possess a vertical axis of rotation. This pattern of flow can be explained by the interaction of a vortex loop with the free surface.

These results provide a mechanism that links the flow fields of adjacent dunes and highlight how dune-related macroturbulence may dominate the entrainment of sediment into both suspended and bedload transport. Additionally, the

mechanism identified here may also be applied to explain the sequence of turbulent events present over other large grain and form roughness in depth-limited alluvial channels.

INTRODUCTION AND AIMS

Dunes are one of the most common alluvial bedforms and have received considerable attention over the past three decades in relation to their occurrence and morphology (e.g. Dinehart, 1989; Gabel, 1993; Dalrymple & Rhodes, 1995; Roden, 1998; Carling, 1999; ten Brinke *et al.*, 1999; Wewetzer & Duck, 1999; Carling *et al.*, 2000a,b), flow dynamics (Jackson, 1976; Müller & Gyr, 1983, 1986, 1996; Yalin, 1992; Kostaschuk & Church, 1993; Lyn, 1993; Nelson *et al.*, 1993; McLean *et al.*, 1994; Bennett & Best, 1995; Kadota & Nezu, 1999; Schmeeckle *et al.*, 1999; Kostaschuk, 2000; Best *et al.*, 2001; Best & Kostaschuk, 2002; Kleinhans, 2002), relationship to sediment transport (Engel & Lam Lau, 1980, 1981; Itakura & Kishi, 1980; Soulsby *et al.*, 1991; Kostaschuk & Ilersich, 1995; Mohrig & Smith, 1996; Bennett & Vendetti, 1997; Villard & Kostaschuk, 1998; Vionnet *et al.*, 1998; Kostaschuk & Villard, 1999; McLean *et al.*, 1999; Shimizu *et al.*, 1999; Vendetti & Bennett, 2000) and effect upon flow resistance (Klaassen, 1979; Wijbenga, 1990; Julien & Klaassen, 1995). Past research has illustrated the nature of the mean and turbulent flow field over sand dunes and shown that these bedforms, which scale with flow depth, are associated with large-scale turbulence or 'macroturbulence' that may be generated over the dune and rise to erupt at the water surface; these eruptions are termed 'boils' by Matthes (1947) and have been the subject of much subsequent work (e.g. Coleman, 1969; Jackson, 1976; Rood & Hickin, 1989; Babakaiff & Hickin, 1996). Both Coleman (1969) and Babakaiff & Hickin (1996) documented the form of these boils as they erupted on the water surface and began to provide indications as to the nature of fluid movement within these macroturbulent coherent structures. Babakaiff & Hickin (1996) related the intensity of eruption of the boil to the relative roughness of the dune, finding that larger dunes produced more intense macroturbulence.

Although macroturbulence has often been associated with flow separation in the lee of steep, angle-of-repose slipface dunes, it has become apparent from studies of low-angle dunes in the field and flume (Smith & McLean, 1977; McLean & Smith, 1979; Kostaschuk & Villard, 1996, 1999; Roden, 1998; Best *et al.*, 2001; Best & Kostaschuk, 2002) that macroturbulence can also be generated by dunes that have much lower angle leeside slopes and possible intermittent flow separation. Additionally, the importance of macroturbulence has been stressed by many authors in relation to the occurrence of dunes and their distinction from other bedforms (e.g. Jackson, 1976; Bennett & Best, 1995, 1996; Best, 1993, 1996; Robert & Ulhman, 2001), as well as to their influence on sediment transport (e.g. Schmeeckle *et al.*, 1999; Vendetti & Bennett, 2000) and the growth of other larger channel topography, such as mid-channel bars (Ashworth *et al.*, 2000). Bennett & Best (1996) hypothesized that the evolution of dunes from a rippled bedstate was associated with the increasing importance of macroturbulence that could penetrate through the entire water depth. They argued that once this occurred, then the subsequent bed-directed inrush of fluid, required to meet continuity to replace the upwelling 'boil', would be sourced from higher in the flow than over ripples and would thus have a higher velocity. They further reasoned that this would subsequently increase the downstream bedload sediment transport rate at the next bedform crest as compared with a rippled bedstate. Recently, Robert & Uhlman (2001) have documented the large increase in turbulence intensity and momentum exchange across the ripple–dune transition and also noted the increased spatial variability in the turbulent flow characteristics as the transition takes place.

Macroturbulence is thus fundamental to dune occurrence and is a common feature visible on the surface of rivers with dune-covered beds. The objective of the current study was thus to examine the *temporal* characteristics of flow over dunes and examine the relationship between macroturbulence generation in the dune leeside and fluid motion at the next downstream crest, to enable

testing of the hypothesis proposed by Bennett & Best (1996). The present study provides qualitative and quantitative evidence of the kinematics and topology of dune-related macroturbulence from two sources:

1 quantitative laboratory results that have been obtained using particle imaging velocimetry (PIV) of whole flow field fluid motions associated with dunes;

2 field observations of the patterns of fluid motion on the river surface above dune-covered beds.

These results provide support for past hypotheses concerning the interactions of dune-related macroturbulence with the outer flow, and allow proposition of a qualitative model of macroturbulence interactions with the water surface that is used to interpret the topology of the macroturbulent structures. This model is of more widespread application in explaining the origin and topology of macroturbulence generated over large-scale bed roughness in depth-limited alluvial channels.

METHODS

Laboratory

Laboratory experiments were conducted in a recirculating hydraulic flume that was 10 m long by 0.30 m deep and 0.30 m wide. The dunes studied were cast in smooth fibreglass and had an identical shape to the angle-of-repose dunes that are fully reported in Bennett & Best (1995). The entire length of the flume was filled with identical fibreglass dunes that were 0.04 m high and 0.63 m wavelength (see schematic layout, Fig. 1A). A steady, uniform flow was then established over these dunes, with the mean velocity over the dune crest being 0.44 m s^{-1} (see Table 1 for mean flow

A: Schematic diagram of flume and fibreglass dunes
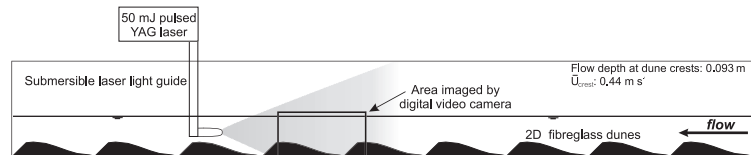
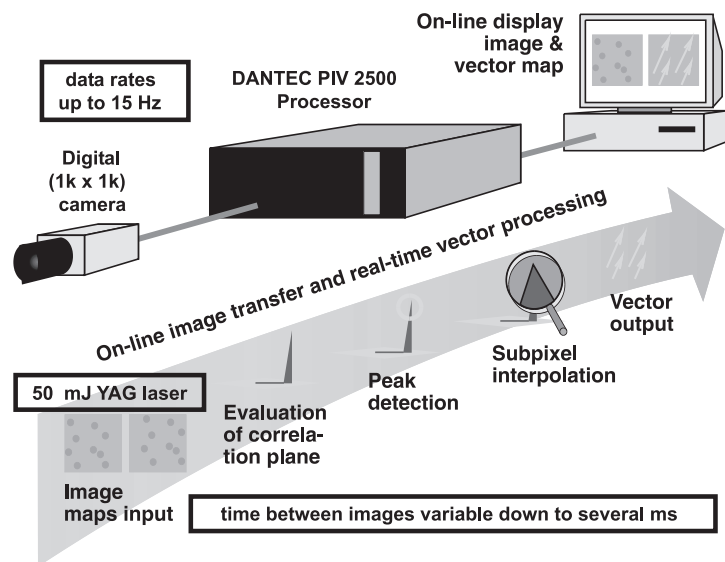### B: Schematic diagram of PIV data collection

Fig. 1 (A) Schematic diagram of the experimental set-up with the bed of the flume covered with identical fibreglass dunes with a morphology identical to those used in Bennett & Best (1995). (B) Schematic flow diagram of the DANTEC particle imaging velocimetry (PIV) system (modified from DANTEC, 2000).

Table 1 Summary of hydraulic conditions and bedform morphology used in this study and that of Bennett & Best (1995).

	This study	Bennett & Best (1995)
Flow depth at crest, Y_{crest} (m)	0.093	0.10
Mean downstream velocity at crest, $\bar{U}_{crest}$ (m s^{-1})	0.44	0.57
Froude number, Fr	0.46 (crest)	0.58 (crest)
Dune wavelength, λ (m)	0.63	0.63
Dune height, h (m)	0.04	0.04

conditions), this being slower than the flow studied by Bennett & Best (1995; Table 1).

Quantification of flow in these experiments was achieved using PIV, which uses the displacement of neutrally buoyant particles over a known time period to track their movement and velocity (see Adrian (1991, 1996) for reviews, and Schmeeckle *et al.* (1999) and Tait *et al.* (1996) for examples of PIV results over dunes and a gravel bed, respectively). Roy *et al.* (1999) and Roy & Buffin-Bélanger (2001) have highlighted the great benefits of utilizing flow visualization combined with multi-point measurements. Their field studies, however, where visualization is far more problematic than in controlled laboratory conditions, used dye visualization and three at-a-point measurements, which, although allowing fuller investigation of the link between velocity time-series and coherent flow structure, were still necessarily limited in their true quantitative scope. Indeed, the use of limited sampling and also choice of threshold criteria for distinguishing turbulent events may encourage the interpretation of two-dimensional structure from what are truly three-dimensional vortices (Smart, 2001). The use of whole flow field PIV overcomes these significant problems and allows quantitative visualization of the flow by monitoring several thousand individual points *simultaneously*. This permits far fuller appreciation of the kinematics of the flow field and reconstruction of the advection and interaction of vortices. The laboratory work reported here represents one of the first applications of this technique to flow over dunes and has many applications to flow over appreciable bed roughness in depth-limited flows.

A DANTEC 2500 PIV system was used in the present study that is capable of providing whole flow field quantification at data rates of up to 15 Hz. Flow seeding was provided by natural impurities in the water and 10 µm titanium-coated mica particles. Two successive digital images are taken of a flow field area, with the images being separated by a short, user-defined interval (here 750 ns). The DANTEC system then calculates the maximum cross-correlation between particle positions in a given interrogation area (e.g. 16×16 pixels) and then uses this maximum correlation peak to produce a mean particle displacement, and hence velocity, for each interrogation area (Fig. 1B). A minimum of six particle pairs is required in each interrogation area in order for the data to be validated. The PIV system can thus produce quantitative whole flow field maps: in this study a two-dimensional plane (*x–y* or horizontal–vertical plane) was examined using one camera; however, use of two cameras can permit quantification of three-dimensional velocities in a two-dimensional plane (DANTEC, 2000). The raw displacement vectors were then filtered to remove large outliers in the data set caused by spurious correlation peaks. Tests showed that a threshold of > 0.9 m s^{-1} was suitable to represent twice the velocity over the crest and this removed less than 2% of the raw vectors, largely near the flow surface where image quality, owing to reflection, was poorer. A moving average of three adjacent pixels was used to yield a data grid with approximately 6500 points in each image. A 50 mJ YAG laser provided a pulsed laser light sheet into the test section through a streamlined submersed light guide (Fig. 1A) that was located 1 m downstream of the test section; the time between laser pulses for these flow conditions was optimized to produce the best validation of velocities (i.e. the time gap should be large enough to allow detectable differences in particle position between images but not so large that the correlation of particles begins to deteriorate) and a time gap of 750 ns between laser pulses was used. In this paper, the flow field in the immediate dune leeside and dune crest were examined (Fig. 2) and data rates of between 1 and 15 Hz were used to examine the mean flow field and the instantaneous flow structure. Each flow field was interrogated using either a 16×16 or 32×32 pixel grid, with between 25 and 50% overlap between
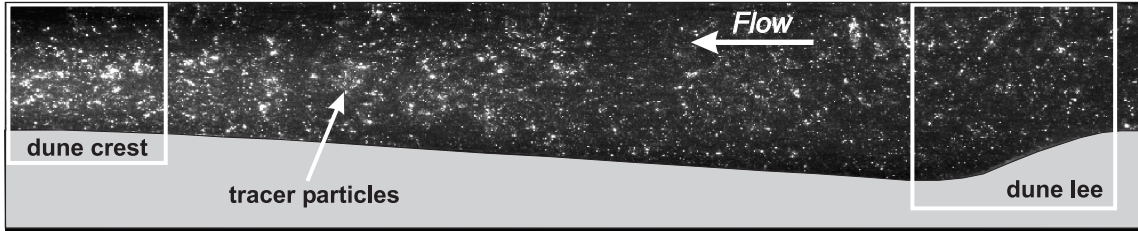
Fig. 2 Particle imaging velocimetry image of the whole experimental dune, with the two areas of study in dune lee and dune crest highlighted. The fields of view are 0.204 m long by 0.205 m deep for the leeside, and 0.148 m wide by 0.149 m deep for the crestal image.

areas and subpixel interpolation to increase the data density (DANTEC, 2000). The mean velocity was derived for each interpolation area and this value was used to calculate the velocity fluctuations and turbulence parameters.

Particle imaging velocimetry can provide an unrivalled method for quantitative visualization of flow, but several factors require care and consideration in the experimental set-up.

1 The system used herein has a maximum sampling rate of 15 Hz, although recent progress has enabled development of PIV that can sample up to 16 kHz for short time periods. The operator can select the sampling frequency and this must be considered at the outset: greater sampling rates require more data storage and thus the length of sample possible is set by the storage available in the PIV processor and the sampling frequency. As each image pair captured is approximately 2 Mb in size, 1 min of data at 15 Hz requires *c.* 1.8 Gb of memory on the processor. Data storage is thus a major consideration in experimental design.

2 Great care is required in illumination of the test section, and reflections from objects or the water surface can cause problems in particle detection.

3 The spatial resolution of measurements is a function of the flow field area imaged and the pixel resolution of the camera, i.e. greater resolution will be obtained by imaging a smaller physical area using the same pixel image size. The operator may thus face a choice depending on the size of the flow field structures of interest: in this study detailed images were taken of the lee and stoss side of the dune that were of a higher spatial resolution than images taken across the entire dune wavelength.

4 Imaging through a moving, and variable height, water surface is difficult owing to refraction of light and changing water depth: this can be solved if a transparent plate can be placed on the surface but this is problematic in experiments such as those reported herein where water surface interactions are important: this problem thus only allowed visualization from the side of the flume in a two-dimensional plane in the experiments reported herein.

Field

Qualitative observations and photographs of turbulent structures associated with flow over natural dune-covered sand-bed rivers were obtained from the surface of the Jamuna River, Bangladesh. Photographs and video records were obtained during high flow stage in August 1994 of flow over 2.5−4-m-high sand dunes in the main channel of the Jamuna River near Bahadurabad, Bangladesh. The flow depth here was *c.* 12 m and the mean flow velocity was *c.* 1.5 m s^{-1}. Further details of this study reach are given in McLelland *et al.* (1999) and Ashworth *et al.* (2000), and details of the dune kinematics and flow fields are given in Roden (1998). The large size of these sand dunes resulted in very large-scale macroturbulence (see the earlier work of Coleman, 1969), with surface boils above large dunes being regular in periodicity (Roden, 1998) and ranging between 5 and 50 m in diameter. As the evolution of the surface eruption of these boils occurred over a period of 5−25 s, detailed observations of video tapes and 35 mm photographs allowed the evolution of these macroturbulent patches and their internal fluid motions to be discerned. The higher sediment concentrations in the surface boils also aided observation of their internal structure.
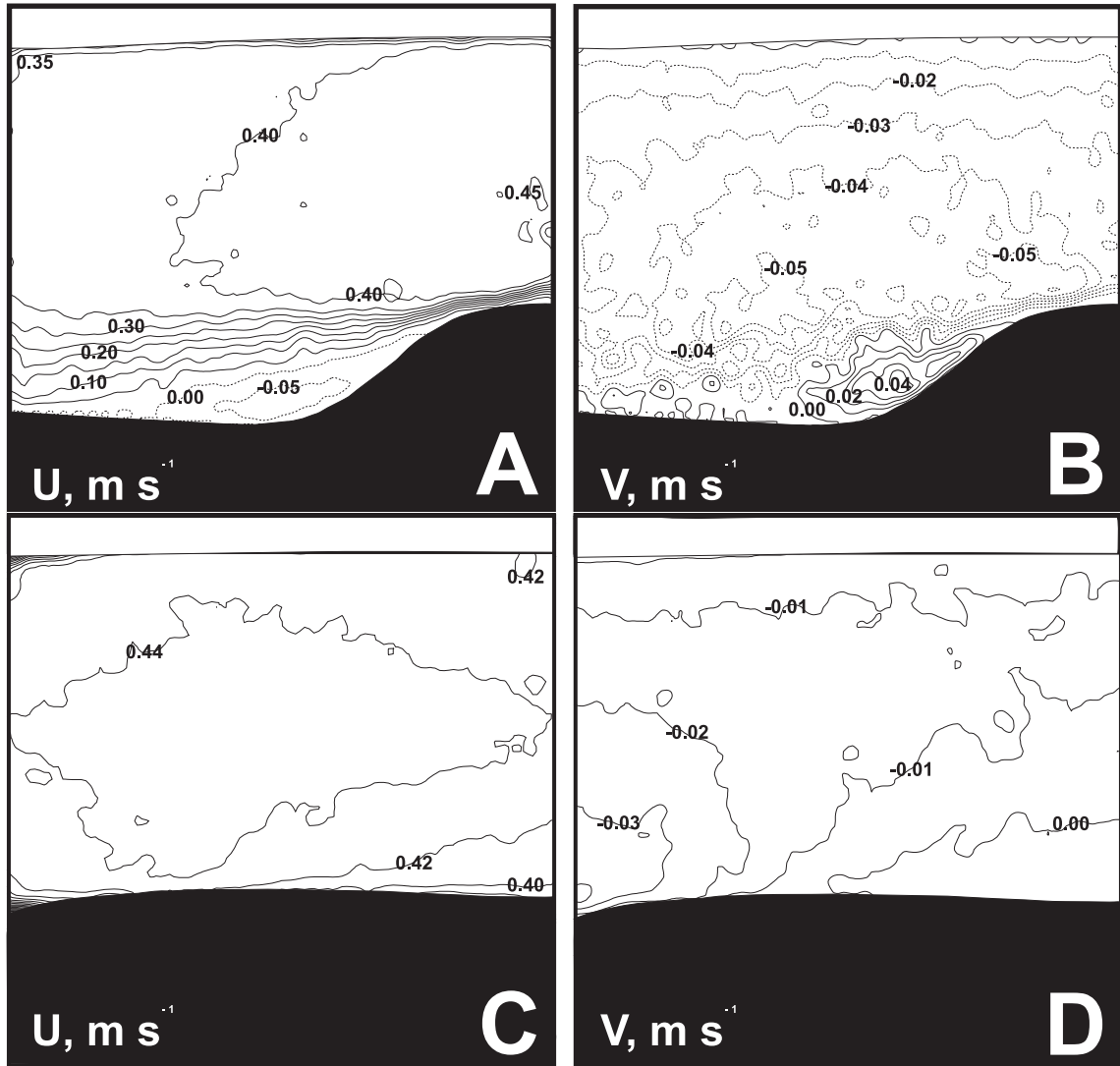
Fig. 3 Mean flow maps for the leeside and crestal regions (see Fig. 2 for location and dimensions of fields of view). (A & B) Mean downstream, *U*, and vertical, *V*, components of flow in the dune leeside. (C & D) Mean downstream, *U*, and vertical, *V*, components of flow over the dune crest. Negative values in (A) and (B) are indicated by dashed contours, and indicate upstream flow and flow towards the bed for the *U* and *V* components respectively.

RESULTS

Laboratory studies of dune macroturbulence

Maps of the mean downstream and vertical velocities in the dune lee (Fig. 3) show the pattern of flow that is normally associated with negative steps and bedforms with steep leesides. Flow deceleration in the leeside (Fig. 3A) is associated with flow separation that produces a recirculating region of fluid that has reverse velocities of up to 0.05 m s^{-1}, with the maximum downstream velocity over the dune crest being *c*. 0.45 m s^{-1}. Vertical velocities (Fig. 3B) show positive values (i.e. fluid moving away from the bed) in the lower part of the leeside flow separation zone (maximum vertical velocity of 0.05 m s^{-1}) but flow directed towards the bed (i.e. negative *v*) over the rest of the flow

depth. Flow over the downstream dune crest (Fig. 3C & D) is far more uniform and the mean flow has largely recovered from the immediate effects of the upstream dune wake. The mean downstream velocity is fairly uniform (Fig. 3C), with the vertical velocity showing the effects of topographic acceleration over the upstream stoss side of the dune and the influence of the next downstream leeside in beginning to direct flow towards the bed over the crest, producing more negative vertical velocities over the crestal region (Fig. 3D).

The pattern of mean flow described above corresponds well with past studies over identical dunes (Bennett & Best, 1995) and also other dune morphologies in both laboratory (Nelson *et al.*, 1993; McLean *et al.*, 1994) and field (Roden, 1998; Kostaschuk, 2000; Best *et al.*, 2001). Figure 4 shows a comparison of three downstream velocity profiles with the data of Bennett & Best (1995) for positions (A) in the dune lee, (B) just downstream of reattachment and (C) on the dune crest, these corresponding to profiles 21, 31 and 68 given by Bennett & Best (1995, fig. 3). The profiles confirm the patterns described above and show a good agreement, especially in the dune lee (Fig. 4A), between the two studies. The PIV system is able to resolve flow closer to the bed than the laser Doppler anemometer (LDA) data reported by Bennett & Best (1995), with the present experiment revealing slightly more near-bed retardation of flow near reattachment, but greater near-bed flow acceleration near the crest (Fig. 3). These small differences may be attributed to both the different mean flow conditions between studies (see Table 1) and any slight non-coincidence of the profiles compared. Nevertheless, the close agreement between these profiles and the mean flow fields demonstrates that similar flow conditions have been investigated herein compared with the comprehensive LDA study of Bennett & Best (1995). The instantaneous
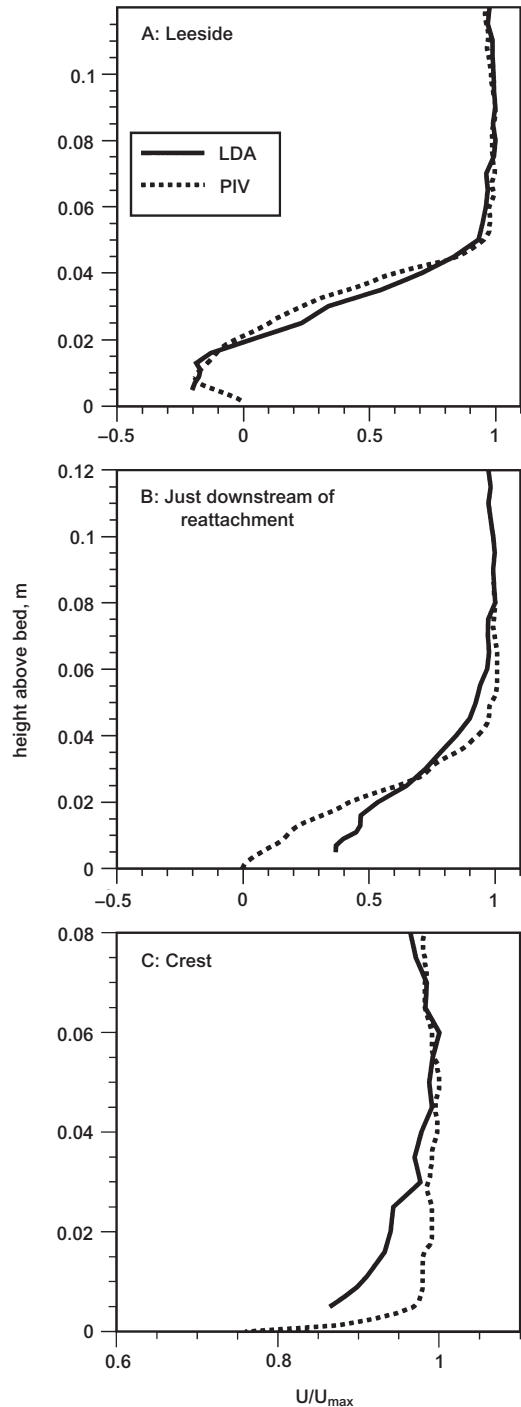
Fig. 4 (*right*) Comparison of downstream velocity profiles at three locations over the dune between this study and the LDA study of Bennett & Best (1995). Profiles are shown for: (A) leeside, (B) just downstream of reattachment and (C) the crestal region, and correspond to profiles 21, 31 and 68 of Bennett & Best (1995). Mean downstream velocity at-a-point, U, is made dimensionless through division by the maximum downstream velocity in the profile, U_{max}.

flow fields quantified in the present study can thus be compared directly to the maps of mean flow and turbulence parameters presented by Bennett & Best (1995).

The broad pattern of flow thus corresponds to expanding, separated flow in the dune lee and this pattern of flow has been shown in many past studies to dominate the production of macroturbulence associated with dunes. These pictures of flow, however, present the *mean* conditions and do not reveal the vital *instantaneous* patterns of flow. Although detailed at-a-point time series can provide abundant information concerning the nature of turbulence (Nelson *et al.*, 1993; McLean *et al.*, 1994; Bennett & Best, 1995; Buffin-Bélanger & Roy, 1998), importantly they cannot provide images of the entire flow field. It is thus often difficult, if not impossible, to relate at-a-point time series to whole flow field motions and the nature of individual turbulent events, their origin and evolution. A unique capability of PIV, however, is the provision of this holistic flow field mapping and the quantitative visualization of evolving coherent structures. In order to display some of the important coherent flow structures associated with dunes, Plates 1 & 2 present images of the motion of coherent flow structures, as shown by regions of high and low velocity flow, in the dune leeside and above the dune crest. Each figure shows a series of whole flow field images at different times over the duration of one coherent flow structure and illustrates maps of downstream velocity, vertical velocity and Reynolds stress. These maps are the first images of their kind ever produced over dune bedforms and show the close interplay between coherent events in the dune boundary layer. A fuller appreciation of these movements, however, is also obtained from animations of the dune flow field, which can be accessed at http://earth.leeds.ac.uk/research/seddies/best/7icfsdunes.htm. The motions associated with each zone are described below.

Dune lee

Fluid motion in the dune lee (Plate 1) is dominated by flow separation that creates a zone of slowly recirculating fluid, which is separated from the freestream flow by a shear layer with high velocity gradient. It is clear, however, that the size of the separation zone varies greatly in time and expands and contracts, this motion depicting the 'flapping' of the shear layer associated with zones of flow separation (e.g. Simpson, 1989; Best & Kostaschuk, 2002). Similar observations have been made by Schmeeckle *et al.* (1999), who noted the difficulty in defining a reattachment point at any one instant. Plate 1 shows one such contraction event where the separation zone, defined by the zero contour, is at its largest at 0 s but then contracts to a minimum at 0.60–0.87 s, before expanding once again. These figures show that the contraction leads to a change in position of the reattachment point (see zero u contour, Plate 1; 0.27–0.60 s), with the zone of downward flow at the bed moving closer to the leeside (e.g. 1.00 s). The contraction of the separation zone appears to coincide with an inrush of fluid towards the upstream crest (see larger patch of bed-directed fluid at crest at 0.27–0.60 s), which subsequently causes contraction of the separation zone, leading to a smaller zone of recirculating flow at 0.87–1.00 s. The nature of this region is thus controlled, in part, by the upstream flow behaviour, which in turn is related to separation zone effects upstream. Hence the nature of the separation zone turbulence and periodicity at one dune is significantly controlled by the temporal turbulent pattern imparted from the upstream bedform.

The modulation of turbulence and destabilization effects of coherent flow structures on separation zone stability have been investigated over negative steps by Mullin *et al.* (1980), and this points to the probable significant interaction between flow fields of dune bedforms. Hence, larger macroturbulence across the ripple–dune transition (Bennett & Best, 1995; Robert & Uhlman, 2001) may lead to the greater interaction between the flow fields of adjacent bedforms and cause greater temporal and spatial variability in the separation zone behaviour. All the maps of Reynolds stress (Plate 1) show that the highest stresses are located within the shear layer, with positive values being associated with the inrush of high velocity fluid towards the bed (quadrant-4 events) (quadrant events are defined by their instantaneous velocities u' and v' (see Best, 1996): quadrant 1, $u' > 0$ and $v' > 0$; quadrant 2, $u' < 0$ and $v' > 0$; quadrant 3, $u' < 0$ and $v' < 0$; quadrant 4, $u' > 0$ and $v' < 0$) and also ejection of lower

momentum fluid into the outer flow (quadrant-2 events). Negative stresses are also high in parts of the leeside shear layer and associated with the ejection of high momentum fluid (quadrant-1 events or outward interactions). The highest stresses in the shear layer, however, are at least up to 40 times greater than in the surrounding fluid and would thus dominate the instantaneous transport of sediment. Temporal variations in the position of the shear layer would thus greatly affect the location of sediment erosion and transport. It is also interesting that the maps of flow within the separation zone (Plate 1) reveal a complex pattern, with the presence of several regions of high and low velocity and Reynolds stress. This supports the previous observations of Schmeeckle *et al.* (1999), who suggested that, at any one given time, the separation zone consists of several large vortices that extend from the shear layer to the bed.

Dune crest

The instantaneous flow fields at the dune crest (Plate 2) are dominated by ejection of low downstream-velocity fluid into the outer flow, which has originated from the upstream dune, and the subsequent reaction of the flow field to this ejection. One such ejection, which occurs over a period of 0.80 s, is shown in Plate 2 and consists of the passage of a zone of low downstream velocity fluid away from the bed (0.13−0.40 s); the region of positive v can be seen to extend up to near the flow surface (0.40 s) with the low u-velocity area becoming more detached from the bed at 0.40 s. This ejection of fluid away from the bed is also associated with significant changes in the temporal signal of the vertical velocity. A distinct area of $-v$ is associated with flow in front of, and behind, the ejection (e.g. 0.27−0.53 s) and reflects the likely three-dimensional topology of flow associated with the ejection. A plot of the ***uv*** vectors at 0.27 s (Fig. 5A) shows the strong bed-directed flow downstream of the region of $+v$, whereas a vector plot of flow at 0.40 s (Fig. 5B) illustrates the strong bed-directed flow upstream of the ejection. This pattern can be explained by considering the reaction of the outer flow to the passage of an ejection. As low-momentum fluid is ejected away from the bed, fluid from higher in the flow is induced to move towards the bed in order
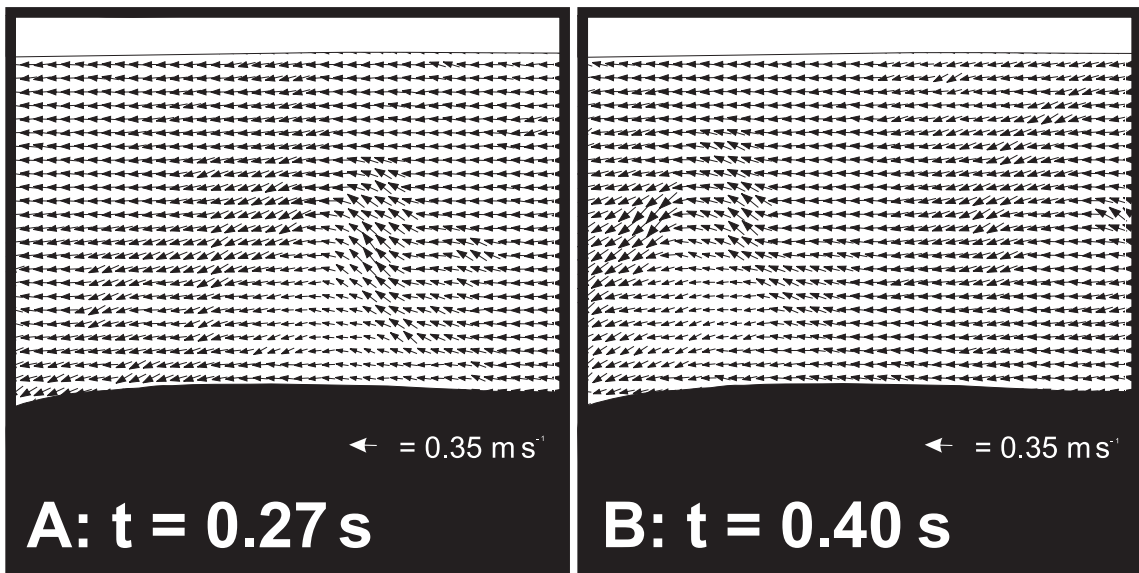

Fig. 5 Plots of ***uv*** vectors for the crestal area at time frames 0.27 and 0.40 s (see Plate 2). Note that the vertical velocities in these vector plots have been multiplied by a factor of five to enable these motions to be visualized. These vector maps illustrate the upward flow associated with the ejection and the flow towards the bed both in front of, and behind, this ejection event.

to satisfy continuity and accounts for the inrush of fluid behind the ejection. These plots provide graphic confirmation of the hypothesis of Bennett & Best (1996) that proposed a link between ejection events and subsequent inrushes sourced from higher in the flow. Additionally, the inrush of flow towards the bed in front (i.e. downstream) of the ejection (Plate 2 & Fig. 5; 0.27–0.53 s) may be explained by considering the likely three-dimensional shape of the ejection (see field observations below and also Schmeeckle *et al.*, 1999, p. 267) that would also cause fluid to be entrained from around the *sides* of the ejection and create a return flow towards the bed as the ejection ascended in the flow. The maps of Reynolds stress (τ_R: Plate 2) also clearly illustrate the dominance of the ejection event through the flow field and that the bed-directed flow in front of the ejection is associated with higher Reynolds stresses (i.e. see higher near-bed τ_R near dune crest at 0.40–0.53 s). The ejection depicted here (Plate 2; 0.27–0.40 s) occupies at least half the flow depth, in good agreement with the observations of Schmeeckle *et al.* (1999).

In order to illustrate further the temporal nature of flow at several points in this flow field, the at-a-point time series in *u*, *v* and τ_R for four points are given in Fig. 6. These points are located (see inset Fig. 6) in mid-flow (1 and 2), near the surface (point 3) and near the bed in close proximity to the dune crest (point 4), and reflect the passage of the ejection shown in Plate 2. Point 1 shows the passage of the ejection that is shown by a marked decrease in *u*, a positive *v* and large τ_R at 0.27 s (Fig. 6; arrowed 'a'). Point 2, located 41 mm downstream of point 1, shows the same response as the ejection advects past this region at 0.33 s (Fig. 6; arrowed 'b'), but additionally shows the strong downflow of fluid towards the bed in front of the advancing ejection at 0.27 s (Fig. 6; arrowed 'c'). Flow near the surface (point 3) also shows the presence of the ejection at a slightly later time (*c.* 0.40 s; Fig. 6; arrowed 'd'), although it is noticeable here that the decrease in *u* is less, the peak in τ_R is much smaller in magnitude than lower in the flow and also there is a lag in the peaks in *v* and τ_R (see label 'd' arrows, Fig. 6). This indicates the significant mixing of the fluid as it rises into this region of higher mean velocity flow and that the peaks in τ_R may be associated with a structure that

is larger here than that present lower in the flow. Point 4, located near the bed, shows a peak in τ_R at *c.* 0.47 s (Fig. 6; arrowed 'e') that is associated with the inrush of flow towards the bed in front (downstream) of the propagating ejection (see Plate 2). Schmeeckle *et al.* (1999) also reported that large-scale vortices frequently break up into smaller scale vortical motions in the mid-stoss region, with only some of the largest vortices advecting through the entire flow depth. Schmeeckle *et al.* (1999) and Shimizu *et al.* (1999) found that this break-up occurs in the region of maximum topographically induced flow acceleration, in a similar position to that documented here. This break-up process, however, will clearly be aided by the inrush events towards the bed documented in the present experiments that are associated with large-scale ejections.

Field observations of water surface structure

Observations, video recordings and series of still photographs of the river surface above dune-covered beds in the Jamuna River allow a summary of the common series of events as large-scale dune-related macroturbulence erupts at the flow surface. These observations complement and extend those previously made by Coleman (1969) in the Jamuna, Jackson (1976) in the Wabash River and Babakaiff & Hickin (1996) in the Squamish River. Photographs from several upwellings on the surface of the Jamuna are shown in Fig. 7, and a summary schematic of the common fluid motions is illustrated in Fig. 8.

The initial eruption of the ejection on the water surface (Fig. 7A; *t* = *c.* 0–3 s, Fig. 8) often appears as a patch of fluid that is upwelling at its rear edge and then downwelling at its downstream front edge. The movement of this fluid thus has a clear axis of rotation in the downstream-spanwise (*x*–*z*) plane and mirrors the observations of Babakaiff & Hickin (1996), who termed this a 'roller structure' (see Fig. 9A). Continued upwelling of the ejection produces an expanding area of upwelling fluid that begins to show a more radial pattern of flow, with the major upwellings being towards the centre of the ejection (Fig. 7B; *t* = *c.* 3–5 s, Fig. 8), but clear downwelling at the front edge. Shear at the edges of this upwelling may begin to generate some rotation in the vertical-spanwise (*y*–*z*)
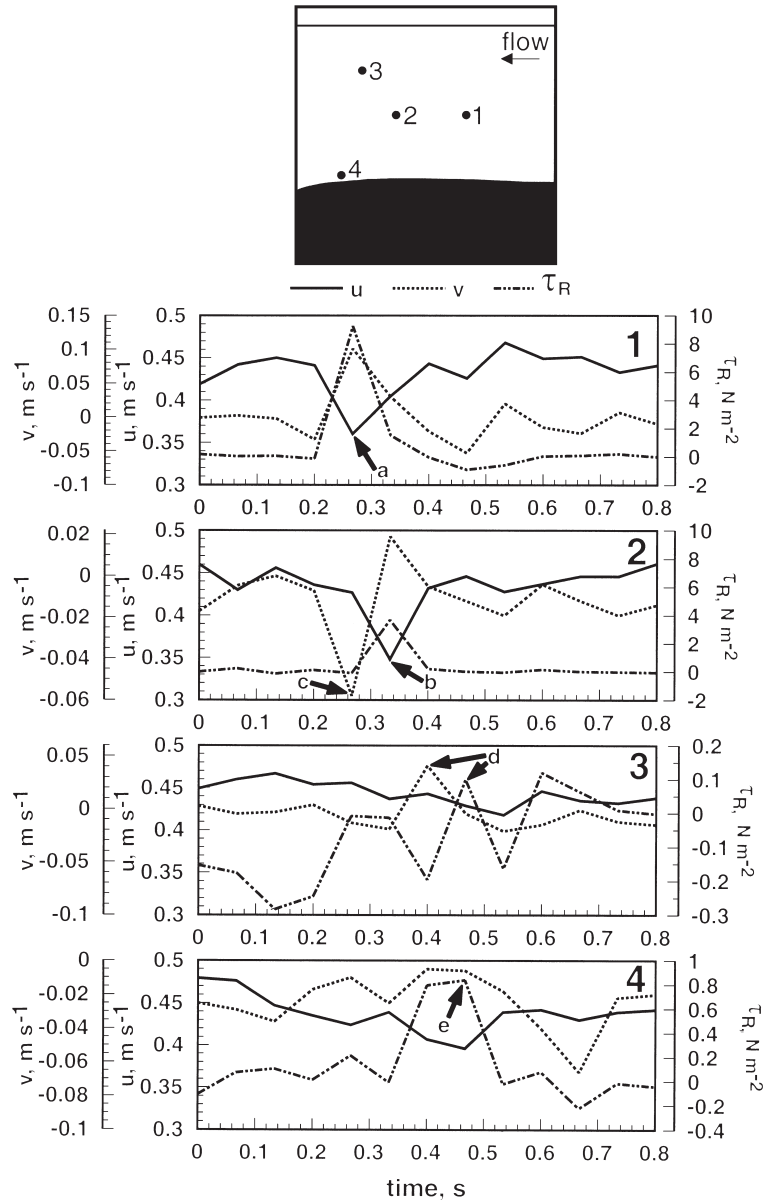
Fig. 6 Time series of instantaneous downstream velocity (*u*), vertical velocity (*v*) and Reynolds Stress (τ_R) for four positions above the dune crest (see inset diagram) for the time periods illustrated on the flow field maps in Plate 2. The arrows on each graph and labels a–e refer to the ejection–inrush event at each point in the flow discussed within the text. Note changing ordinate scales for *v* and τ_R between graphs.

plane (*t* = *c*. 5 s; Fig. 8). In the photographs of the Jamuna shown here, an opposing slight wind encouraged development of distinct waves, up to *c*. 0.3 m high, at the downstream edge of the upwelling (Fig. 7C & D; *t* = *c*. 1–5 s, Fig. 8). At this stage, a vertical vorticity also begins to be well-developed both at the edges of the upwelling, owing to shear with the surrounding flow (Fig. 7E; *t* = *c*. 5–10 s, Fig. 8), and also at the trailing edge of

the upwelling where distinct, separate vortices with a vertical axis of rotation start to form (*t* = *c*. 10 s; Fig. 8). The rotation direction of these vertical vortices on each side of the upwelling often tends to be in towards the upwelling (*t* = *c*. 10 s; Fig. 8), this again mirroring the observation of Babakaiff & Hickin (1996; Fig. 9A) who observed 'horns' associated with surface macroturbulence that also rotated in towards the upwelling ejection event.
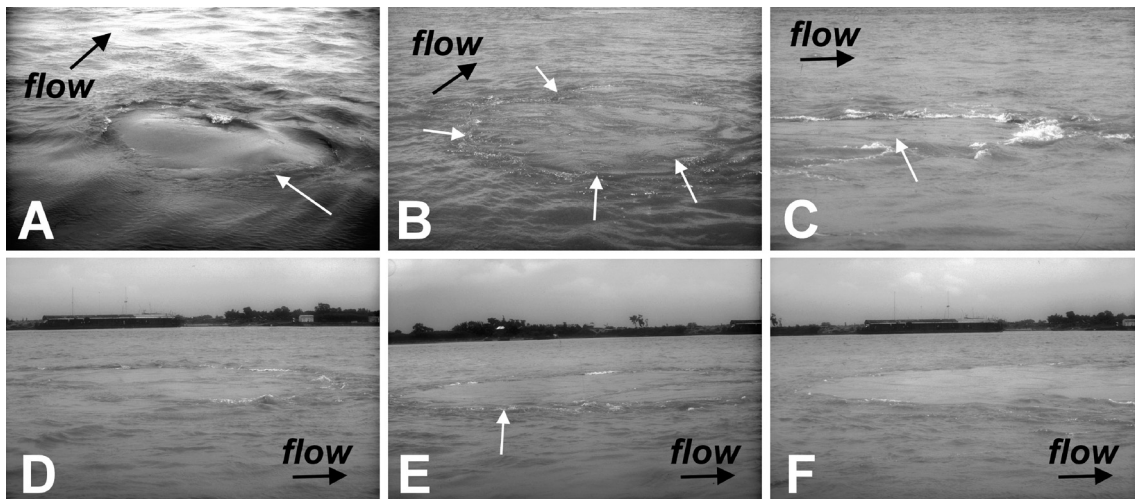
Fig. 7 Photographs of vortex–free-surface interactions in the Jamuna River, Bangladesh. (A–D) are images of separate events whereas (E) and (F) show the same boil. (A) Initial upwelling showing water surface waves on downflow side of boil. Width of image *c.* 4 m. (B) Complex upwelling with multiple points of upwelling (arrowed). Width of image *c.* 8 m. (C) Violent upwelling (arrowed) and development of strong water surface waves at downflow side of boil. Width of image *c.* 3 m. (D) Water surface waves around large boil that is *c.* 30 m wide. (E & F) Two images taken approximately 5 s apart showing final stage of development of a large-scale eruption which at its maximum reaches *c.* 30−35 m across. (E) Large boil on the water surface with developing vertical vortices (arrowed) and diminishing water surface waves. (F) Boil eruption wanes further and the event begins to lose its distinct water surface expression.

Continued development of the ejection (Fig. 7F; $t = c.$ 15 s, Fig. 8) sees further radial expansion of the patch of upwelling fluid, although the intensity of upwelling decreases and shear at its edges produces a series of smaller vortices with a vertical axis of rotation. The larger vertical vortices generated to the back and rear of the upwelling also at first increase, but then decrease, in their size and rotational velocity as the upwelling continues ($t = c.$ 15 s; Fig. 8). Dissipation of the upwelling causes these features to become more indistinct until the eruption is finished. The width on the water surface of these upwellings associated with dune-related macroturbulence ranged from 5 to approximately 50 m in the Jamuna River.

DISCUSSION: THE TOPOLOGY OF DUNE-RELATED MACROTURBULENCE

These results of PIV quantification of the whole flow field dynamics associated with sand dunes and synthesis of observations of macroturbulence–water-surface interactions above natural dune-covered sand beds—reveal four key features.

1 The shear layer and separation zone associated with dunes are spatially and temporally dynamic, and 'flapping' of the shear layer may be caused and modulated by turbulent coherent flow structures generated upstream.

2 Reynolds stresses in the leeside are dominated by the free shear layer associated with the separation zone in dunes with angle-of-repose leesides.

3 Ejections of low downstream-momentum fluid away from the bed dominate the instantaneous flow field over the crestal regions of the dune. These ejections create return flows towards the bed both in front of, and behind, the ejection. The highest instantaneous Reynolds stresses are associated with these ejections and inrushes (quadrant 2 and 4 events respectively).

4 Although the water surface over a dune field does show a great variability in the patterns of upwellings or 'boils' associated with dunes, a common pattern can be discerned that consists of a central upwelling that has a spanwise axis
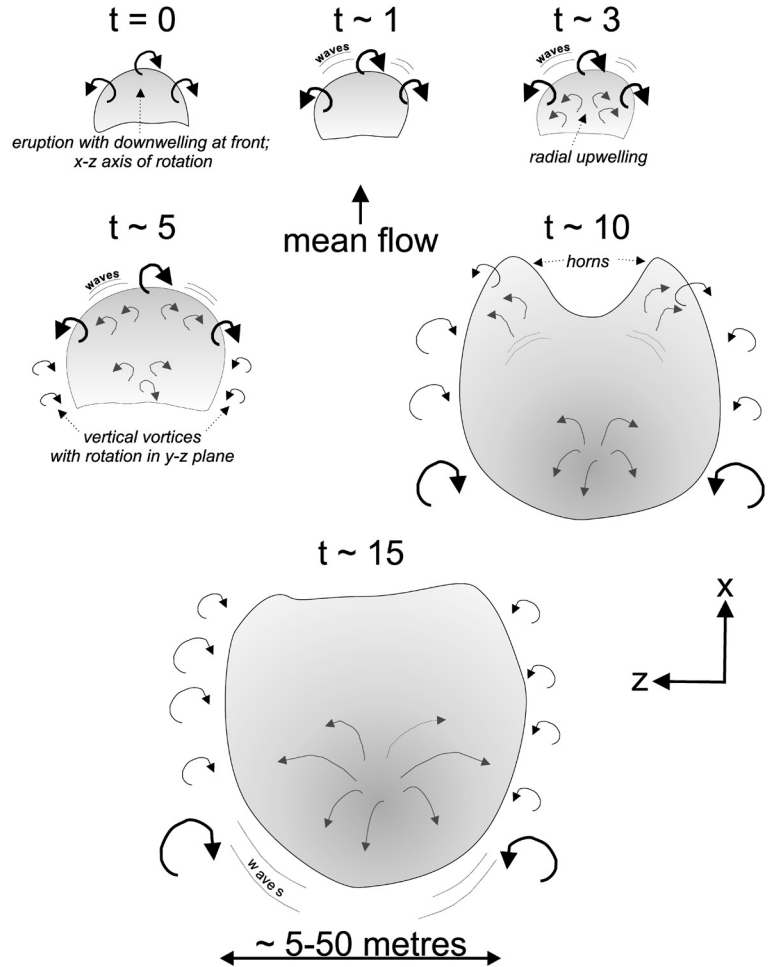
Fig. 8 Sketches of the patterns of flow associated with eruption of ejections onto the water surface, Jamuna River, Bangladesh. These sketches represent a summary of still and video photography over a number of large sand dunes and depict the most commonly observed sequence of events: *t*, time from start of boil eruption (s). These surface boils can reach up to 50 m in diameter over the largest sand dunes. *x*, *y* and *z* refer to downstream, vertical and transverse axes respectively.

of rotation and is later associated with secondary vortices that possess a vertical axis of rotation.

Previous work examining the coherent flow structures associated with dunes (Müller & Gyr, 1986; Nezu & Nakagawa, 1993; Kadota & Nezu, 1999) has suggested that in three dimensions these structures have a loop or horseshoe morphology (Fig. 9B & C), although these studies show that such vorticity can arise either along the shear layer or from the reattachment region (Fig. 9B & C), a feature also observed in the present experiments. Acarlar & Smith (1987) also demonstrated a similar morphology for vortices generated at low flow Reynolds number downstream of hemispherical obstacles. Such three-dimensional vortices may be more easily attained over bedforms that

have a sinuous crestline that encourage production of vortices with a limited spanwise extent. Experimental work has shown how leeside flow associated with cylinders (Délery, 2001) and rectangular roughness (Fig. 9D; Martinuzzi & Tropea, 1993) may also lead to production of a flow structure associated with the separation zone that has a distinct 'horseshoe' morphology and thus could be expected to shed structures with a 'loop' shape.

Additionally, work on the interactions between coherent flow structures with a free surface (e.g. Rashidi & Banerjee, 1988; Rood, 1995; Sarpkaya, 1996; Kumar *et al.*, 1998) has included focus on the interaction of a vortex loop with a free surface (see Sarpkaya, 1996). This work has shown the initial contact of the loop head with the free
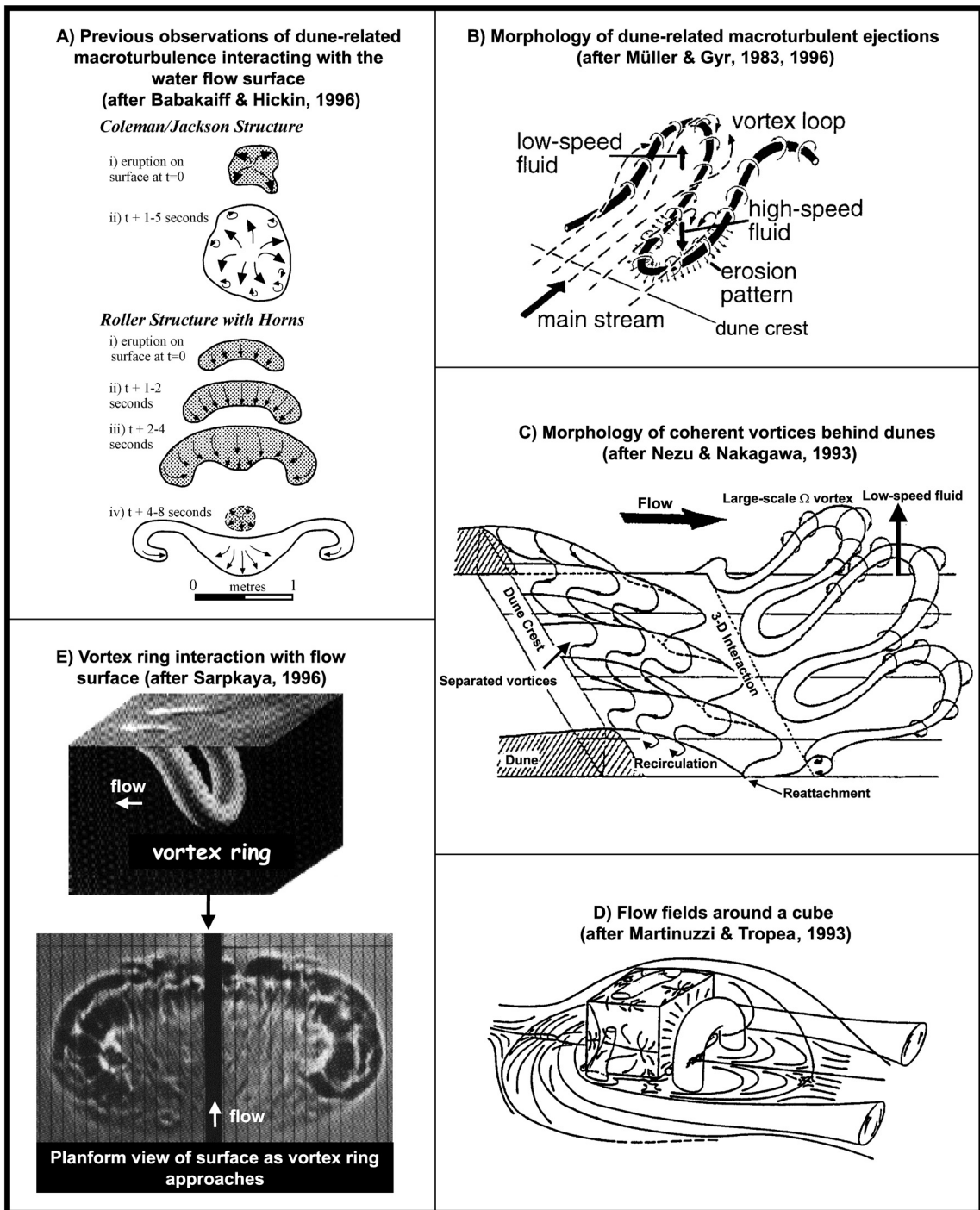
Fig. 9 Vorticity associated with dunes and surface obstructions, and vortex interactions with a free surface. (A) Evolution of boils on the water surface (from Babakaiff & Hickin (1996) and after Coleman (1969) and Jackson (1976)). (B) Three-dimensional flow around a boil and the structure of dune-related macroturbulence proposed by Müller & Gyr (1983, 1986, 1996). (C) The morphology of coherent vortices behind dunes (after Nezu & Nakagawa, 1993). (D) Vortex systems associated with flow around a surface-mounted cube (after Martinuzzi & Tropea, 1993). (E) Interactions of a vortex ring with the free surface (after Sarpkaya, 1996): vortex legs interacting with the surface (upper) and plan view of loop vortex approaching surface (lower).

surface (Fig. 9E) and that as the loop continues to rise then the legs of the vortex loop become connected to the free surface (Fig. 9E). This pattern of large-scale connection of the vortex loop head with an *x–z* axis of rotation, which is followed by emergence of vertical vortices with a *y–z* axis of rotation, bears striking similarity to the observations made on the surface of rivers with dune-covered beds. These observations suggest that the common topology of macroturbulence associated with dunes with distinct flow separation zones may be a vortex loop that, when interacting with the water surface, provides an interaction similar to that of classical vortex loops. This similarity of interaction allows proposition of a conceptual model to explain the patterns of upwelling observed on the water surface above dune beds (Fig. 10).

Once the vortex has been generated and shed into the outer flow, possibly assisted by flapping of the shear layer, which will aid expulsion of the ejection, the vortex approaches the surface (Fig. 10A). The first interaction of the ejection with the surface occurs as the head of the vortex loop encounters the surface, this producing an upwelling on the flow surface on the upflow side of the vortex and a downwelling on its downflow margin (Fig. 10B). As the eruption continues (Fig. 10C) the legs of the loop vortex interact with, and become connected to, the flow surface (see Sarpkaya, 1996; Kumar *et al.*, 1998), producing vortices with a vertical axis of rotation. Continued eruption at the centre of the vortex produces an upwelling in its centre and shear with the surrounding flow also produces secondary vortices,
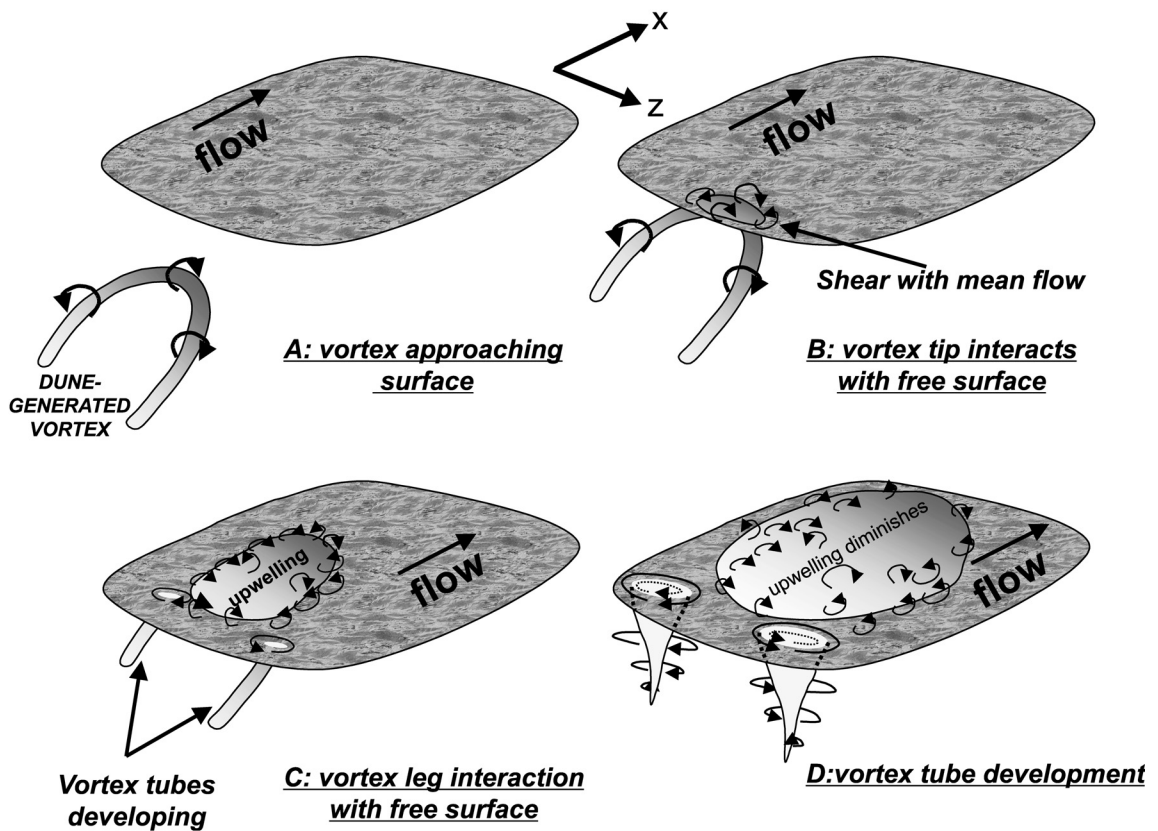

Fig. 10 A schematic model of flow to illustrate the interaction of dune-related macroturbulence with the water surface. This three-dimensional sketch illustrates the various stages of interaction of the boil with the flow surface: however, this interaction will also be associated with the inrush of fluid back towards the bed as quantified in the laboratory PIV experiments.

with vertical axes, at the edges of the main boil (Fig. 10C & D). As the upwelling continues, the velocity of the ejection decreases and the boil begins to diminish in intensity, with the vertical vortices of the legs of the vortex loop also enlarging in size but decreasing in rotational velocity (Fig. 10D).

This general pattern of flow can be observed on the water surface over most dune-covered beds, and extends previous visual observations of boil morphology (e.g. Jackson, 1976; Babakaiff & Hickin, 1996). These macroturbulent events are well-known to be a dominant mechanism for the suspension of sediment over dune beds (Jackson, 1976; Lapointe, 1992; Shimizu *et al.*, 1999; Schmeeckle *et al.*, 1999; Vendetti & Bennett, 2000) and in the present study were visually associated with higher quantities of suspended sediment that can quantitatively be linked to higher sediment concentrations in the Jamuna (Roden, 1998). Another significant corollary of the macroturbulent ejections demonstrated here, however, is their significant influence on inrushes of fluid towards the bed that are required to satisfy continuity (Plate 2). This mechanism of surface interaction has also been proposed in other studies to possibly induce subsequent inrushes (Rashidi & Banerjee, 1988), and these may dominate the instantaneous Reynolds stresses and bed sediment transport. The role of the ejection–inrush sequence may thus be vital in increasing sediment transport rates over the dune and in causing the ripple–dune transition (Bennett & Best, 1996). Additionally, it is also clear that the spatial variability in flow is greater over a dune bed (Robert & Uhlman, 2001) and this may aid the ripple–dune transition.

The present results also lend support to past work that has highlighted the importance of quadrant-4 events in dominating bedload sediment transport (Nelson *et al.*, 1995). This ejection–inrush process, and the series of events outlined here, may also be expected to be important over other types of large-scale bed roughness in alluvial channels. For instance, in gravel-bed rivers this process may provide a mechanism to explain the high and low speed 'wedges' of flow observed by Buffin-Bélanger & Roy (1998), Buffin-Bélanger *et al.* (2000) and Roy & Buffin-Bélanger (2001). These authors have described observations of eddy shedding associated with pebble clusters and

proposed that the flow is dominated by a series of low and high speed 'wedges', of low frequency (*c.* 0.15 Hz), with the high-speed wedges being dominant in producing large bed shear stresses, which were reasoned to be the key element in sediment transport (Buffin-Bélanger *et al.*, 2000). However, these representations of the flow field were based on only three simultaneous measurements that each had a sampling volume of approximately 0.1 Y, which makes interpretation of the precise flow structure and the behaviour of *individual* turbulent events problematic. The present study has yielded a holistic picture of flow that provides a mechanism to explain these previous observations. Wedges of low-speed flow, produced by ejection/flapping of the shear layer, are followed by the inrush of high-speed wedges from the outer flow, which, because they move towards the bed from the outer flow, arrive later at the bed than higher in the boundary layer.

The visualizations shown here (Plate 2) may be used to provide a mechanism to explain the pattern of *u* and *v* signals presented by Ferguson *et al.* (1996) and flow patterns conjectured by Yalin (1992). Buffin-Bélanger *et al.* (2000) and Roy & Buffin-Bélanger (2001) highlight, however, that there is often no discernible pattern to the quadrant structure in their time series. The present study suggests how this may reflect the complex three-dimensional topology of the coherent flow structures that will produce varying quadrant signatures depending on how they translate through any measurement volume. The response of the flow to ejection and shear layer flapping will involve a three-dimensional flow around the ejection that will induce inrushes both in front of, and behind, the advecting ejection (Plate 2). Future PIV work will focus on the two- and three-dimensional flow field of dunes and grain roughness to fully quantify the characteristics of this macroturbulence, which may often dominate the entire boundary layer in depth-limited flows.

ACKNOWLEDGEMENTS

NOMENCLATURE

Fr Froude number ($=\bar{U}_{crest}/\sqrt{g}Y_{crest}^{0.5}$)

g gravitational acceleration (m s^{-1} s^{-1})

h dune height (m)

t time (s)

u instantaneous downstream velocity at-a-point (m s^{-1})

u' deviation of instantaneous downstream velocity from mean ($= u - U$; m s^{-1})

U mean downstream velocity at-a-point (m s^{-1})

$\bar{U}_{crest}$ mean downstream velocity at dune crest (m s^{-1})

U_{max} maximum downstream velocity in a vertical profile (m s^{-1})

v instantaneous vertical velocity at-a-point (m s^{-1})

v' deviation of instantaneous vertical velocity from mean ($= v - V$; m s^{-1})

V mean vertical velocity at-a-point (m s^{-1})

Y flow depth (m)

Y_{crest} flow depth at dune crest (m)

λ dune wavelength (m)

ρ fluid density (kg m^{-3})

τ_R Reynolds stress ($\tau_R = -\rho\,\overline{u'v'}$; N m^{-2})

x, y and z refer to the downstream, vertical and transverse axes respectively.

REFERENCES

Acarlar, M.S. and Smith, C.R. (1987) A study of hairpin vortices in a laminar boundary layer. Part 1. Hairpin vortices generated by a hemispherical protuberance. *J. Fluid. Mech.*, **175**, 1–41.

Adrian, R.J. (1991) Particle-imaging techniques for experimental fluid dynamics. *Ann. Rev. Fluid Mech.*, **23**, 261–304.

Adrian, R.J. (1996) Laser velocimetry. In: *Fluid Mechanics Measurements* (Ed. R.J. Goldstein), pp. 175–299, Taylor and Francis, London.

Ashworth, P.J., Best, J.L., Roden, J., Bristow, C.S. and Klaassen, G.J. (2000) Morphological evolution and dynamics of a large, sand braid-bar, Jamuna River, Bangladesh. *Sedimentology*, **47**, 533–555.

Babakaiff, C.S. and Hickin, E.J. (1996) Coherent flow structures in Squamish River Estuary, British Columbia, Canada. In: *Coherent Flow Structures in Open Channels* (Eds P.J. Ashworth, S.J. Bennett, J.L. Best and S.J. McLelland), pp. 321–342. Wiley, Chichester.

Bennett, S.J. and Best, J.L. (1995) Mean flow and turbulence structure over fixed, two-dimensional dunes: implications for sediment transport and dune stability. *Sedimentology*, **42**, 491–513.

Bennett, S.J. and Best, J.L. (1996) Mean flow and turbulence structure over fixed ripples and the ripple-dune transition. In: *Coherent Flow Structures in Open Channels* (Eds P.J. Ashworth, S.J. Bennett, J.L. Best and S.J. McLelland), pp. 281–304. Wiley, Chichester.

Bennett, S.J. and Vendetti, J. (1997) Turbulent flow and suspended sediment transport over fixed dunes. In: *Proceedings, Conference on Management of Landscapes Disturbed by Channel Incision* (Eds S.S.Y. Wang, E.J. Langendoen and F.D. Shields, Jr), pp. 949–954. Center for Computational Hydroscience and Engineering, University of Mississippi, Oxford, USA.

Best, J.L. (1993) On the interactions between turbulent flow structure, sediment transport and bedform development: some considerations from recent experimental research. In: *Turbulence: Perspectives on Flow and*

Sediment Transport (Eds: N.J. Clifford, J.R. French and J. Hardisty), pp. 61–92. Wiley, Chichester.

Best, J.L. (1996) The fluid dynamics of small-scale alluvial bedforms. In: *Advances in Fluvial Dynamics and Stratigraphy* (Eds P.A. Carling and M.R. Dawson), pp. 67–125. Wiley, Chichester.

Best, J.L. and Kostaschuk, R.A. (2002) An experimental study of turbulent flow over a low-angle dune. *J. Geophys. Res.*, **107**(C9), 3135–3154.

Best, J.L., Kostaschuk, R.A. and Villard, P.V. (2001) Quantitative visualization of flow fields associated with alluvial sand dunes: results from the laboratory and field using ultrasonic and acoustic Doppler anemometry. *J. Vizualization*, **4**, 373–381.

Buffin-Bélanger, T. and Roy, A.G. (1998) Effects of a pebble cluster on the turbulent structure of a depth-limited flow in a gravel-bed river. *Geomorphology*, **25**, 249–267.

Buffin-Bélanger, T., Roy, A.G. and Kirkbride, A.D. (2000) On large-scale flow structures in a gravel-bed river. *Geomorphology*, **32**, 417–435.

Carling, P.A. (1999) Subaqueous gravel dunes. *J. Sediment. Res.*, **69**, 534–545.

Carling, P.A., Gölz, E., Orr, H.G. and Radecki-Pawlik, A. (2000a) The morphodynamics of fluvial sand dunes in the River Rhine near Mainz, Germany, Part I: sedimentology and morphology. *Sedimentology*, **47**, 227–252.

Carling, P.A., Williams, J.J., Gölz, E. and Kelsey, A.D. (2000b) The morphodynamics of fluvial sand dunes in the River Rhine near Mainz, Germany, Part II: hydrodynamics and sediment transport. *Sedimentology*, **47**, 253–278.

Coleman, J.M. (1969) Brahmaputra River: channel processes and sedimentation. *Sediment. Geol.*, **3**, 129–239.

Dalrymple, R.W. and Rhodes, R.N. (1995) Estuarine dunes and bars. In: *Geomorphology and Sedimentology of Estuaries* (Ed. G.M.E. Perillo), pp. 359–422. Elsevier, Amsterdam.

DANTEC (2000) *FlowMap Particle Image Velocimetry Instrumentation, Installation and Users Guide*. DANTEC, Lyngby, Denmark.

Délery, J.M. (2001) Robert Legendre and Henri Werlé: toward the elucidation of three-dimensional separation. *Annu. Rev. Fluid Mech.*, **33**, 129–154.

Dinehart, R.L. (1989) Dune migration in a steep, coarse-bedded stream. *Water Resour. Res.*, **25**, 911–923.

Engel, P. and Lam Lau, Y. (1980) Computation of bed load using bathymetric data, *J. Hydraul. Div., ASCE*, **106**, 369–380.

Engel, P. and Lam Lau, Y. (1981) Bed load discharge coefficient, *J. Hydraul. Div., ASCE*, **106**, 1445–1454.

Ferguson, R.I., Kirkbride, A.D. and Roy, A.G. (1996) Markov analysis of velocity fluctuations in gravel-bed rivers. In: *Coherent Flow Structures in Open Channels* (Eds P.J. Ashworth, S.J. Bennett, J.L. Best and S.J. McLelland), pp. 165–183. Wiley, Chichester.

Gabel, S.L. (1993) Geometry and kinematics of dunes during steady and unsteady flows in the Calamus River, Nebraska, USA. *Sedimentology*, **40**, 237–269.

Itakura, T. and Kishi, T. (1980) Open channel flow with suspended sediment on sand waves. In: *Proceedings of the Third International Symposium on Stochastic Hydraulics* (Eds H. Kikkawa and Y. Iwasa), pp. 599–609. Tokyo

Jackson, R.G. (1976) Sedimentological and fluid-dynamic implications of the turbulence bursting phenomenon in geophysical flows, *J. Fluid Mech.*, **77**, 531–560.

Julien, P.Y. and Klaassen, G.J. (1995) Sand–dune geometry of large rivers during flood. *J. Hydraul. Eng.*, **121**, 657–663.

Kadota, A. and Nezu, I. (1999) Three-dimensional structure of space–time correlation on coherent vortices generated behind dune crest, *J. Hydraul. Res.*, **37**, 59–80.

Klaassen, G.J. (1979) *Sediment Transport and Hydraulic Roughness in Relation to Bed Forms*. Publication 213, Delft Hydraulics, Delft, 33 pp.

Kleinhans, M.G. (2002) Sorting out sand and gravel: sediment transport and deposition in sand–gravel bed rivers. PhD Thesis, Royal Dutch Geographical Society/Faculty of Geographical Sciences, Utrecht University. *Neth. Geogr. Stud.*, **293**, 317 pp.

Kostaschuk, R.A. (2000) A field study of turbulence and sediment dynamics over subaqueous dunes with flow separation. *Sedimentology*, **47**, 519–531.

Kostaschuk, R.A. and Church, M.A. (1993) Macroturbulence generated by dunes: Fraser River, Canada. *Sediment. Geol.*, **85**, 25–37.

Kostaschuk, R.A. and Ilersich, S.A. (1995) Dune geometry and sediment transport: Fraser River, British Columbia. In: *River Geomorphology* (Ed. E.J. Hickin), pp. 19–36. Wiley, Chichester.

Kostaschuk, R.A. and Villard, P.V. (1996) Flow and sediment transport over large subaqueous dunes: Fraser River, Canada. *Sedimentology*, **43**, 849–863.

Kostaschuk, R.A. and Villard, P.V. (1999) Turbulent sand suspension over dunes. In: *Fluvial Sedimentology VI* (Eds N.D. Smith and J. Rogers). *Spec. Publs Int. Assoc. Sedimentol.*, **28**, 3–14.

Kumar, S., Gupta, R. and Banerjee, S. (1998) An experimental investigation of the characteristics of free-surface turbulence in channel-flow. *Phys. Fluids*, **10**, 437–456.

Lapointe, M. (1992) Burst-like sediment suspension events in a sand bed river. *Earth Surf. Process. Landf.*, **17**, 253–270.

Lyn, D.A. (1993) Turbulence measurements in open-channel flows over artificial bedforms. *J. Hydraul. Eng.*, **119**, 306–326.

Martinuzzi, R. and Tropea, C. (1993) The flow around surface-mounted, prismatic obstacles placed in a fully developed channel flow. *J. Fluids Eng.*, **115**, 85–92.

Matthes, G.H. (1947) Macroturbulence in natural stream flow. *Trans. Am. Geophys. Union*, **28**, 255−262.

McLean, S.R. and Smith, J.D. (1979) Turbulence measurements in the boundary layer over a sand wave field. *J. Geophys. Res.*, **84**, 7791−7808.

McLean, S.R., Nelson, J.M. and Wolfe, S.R. (1994) Turbulence structure over two-dimensional bedforms: implications for sediment transport. *J. Geophys. Res.*, **99**, 12729−12747.

McLean, S.R., Wolfe, S.R. and Nelson, J.M. (1999) Predicting boundary shear stress and sediment transport over bedforms. *J. Hydraul. Eng.*, **125**, 725−736.

McLelland, S.J., Ashworth, P.J., Best, J.L., Roden, J. & Klaassen, G.J. (1999) Flow structure and spatial distribution of suspended sediment around an evolving braid bar, Jamuna River, Bangladesh. In: *Fluvial Sedimentology VI* (Eds N.D. Smith and J. Rogers). *Spec. Publs Int. Assoc. Sedimentol.*, **28**, 43−57.

Mohrig, D. and Smith, J.D. (1996) Predicting the migration rates of subaqueous dunes. *Water Resour. Res.*, **10**, 3207−3217.

Müller, A. and Gyr, A. (1983) Visualisation of the mixing layer behind dunes. In: *Mechanics of Sediment Transport* (Eds B.M. Sumer and A. Müller), pp. 41−45. A.A. Balkema, Rotterdam.

Müller, A. and Gyr, A. (1986) On the vortex formation in the mixing layer behind dunes. *J. Hydraul. Res.*, **24**, 359−375.

Müller, A. and Gyr, A. (1996) Geometrical analysis of the feedback between flow, bedforms and sediment transport. In: *Coherent Flow Structures in Open Channels* (Eds P.J. Ashworth, S.J. Bennett, J.L. Best and S.J. McLelland), pp. 237−247. Wiley, Chichester.

Mullin, T., Greated, C.A. and Grant, I. (1980) Pulsating flow over a step. *Phys. Fluids*, **23**, 669−674.

Nelson, J.M., McLean, S.R. and Wolfe, S.R. (1993) Mean flow and turbulence fields over two-dimensional bedforms. *Water Resour. Res.*, **29**, 3935−3953.

Nelson, J.M., Shreve, R.L., McLean, S.R. and Drake, T.G. (1995) Role of near-bed turbulence structure in bed load transport and bed form mechanics. *Water Resour. Res.*, **31**, 2071−2086.

Nezu, I. and Nakagawa, H. (1993) Three-dimensional structures of coherent vortices generated behind dunes in turbulent free-surface flows. In: *Proceedings, 5th International Symposium on Refined Flows Modelling and Turbulence Measurements*, pp. 603−612.

Rashidi, M. and Banerjee, S. (1988) Turbulence structure in free-surface channel flows. *Phys. Fluids*, **31**, 2492−2503.

Robert, A. and Uhlman, W. (2001) An experimental study on the ripple−dune transition. *Earth. Surf. Proc. Landf.*, **26**, 615−629.

Roden, J.E. (1998) The sedimentology and dynamics of mega-dunes, Jamuna River, Bangladesh. Unpublished PhD thesis, Department of Earth Sciences and School of Geography, University of Leeds, 310 pp.

Rood, E.P. (1995) Free-surface vorticity. In: *Fluid Vortices* (Ed. S. Green), pp. 687−730. Kluwer, Norwell, MA.

Rood, K.M. and Hickin, E.J. (1989) Suspended sediment concentration in relation to surface-flow structure in Squamish River estuary, southwestern British Columbia. *Can. J. Earth Sci.*, **26**, 2172−2176.

Roy, A.G. and Buffin-Bélanger, T. (2001) Advances in the study of turbulent flow structures in gravel-bed rivers. In: *Gravel-bed Rivers V* (Ed. M.P. Mosley), pp. 375−397. New Zealand Hydrological Society, Wellington.

Roy, A.G., Biron, P., Buffin-Bélanger, T. and Levasseur, S. (1999) Combined visual and quantitative techniques in the study of natural flows. *Water Resour. Res.*, **35**, 871−877.

Sarpkaya, T. (1996) Vorticity, free surface, and surfactants. *Ann. Rev. Fluid Mech*, **28**, 83−128.

Schmeeckle, M.W., Shimizu, Y., Hoshi, K., Baba, H. and Ikezaki, S. (1999) Turbulent structures and suspended sediment over two-dimensional dunes. In: *River, Coastal and Estuarine Morphodynamics, Proceedings International Association for Hydraulic Research Symposium*, pp. 261−270. Genova, September.

Shimizu, Y., Schmeeckle, M.W., Hoshi, K. and Tateya, K. (1999) Numerical simulation of turbulence over two-dimensional dunes. In: *River, Coastal and Estuarine Morphodynamics, Proceedings International Association for Hydraulic Research Symposium*, pp. 251−260. Genova, September.

Simpson, R.L. (1989) Turbulent boundary-layer separation. *Ann. Rev. Fluid Mech.*, **21**, 205−234.

Smart, G.M. (2001) Discussion of 'Advances in the study of turbulent flow structures in gravel-bed rivers' by Roy, A.G. and Buffin-Bélanger, T. In: *Gravel-bed Rivers V* (Ed. M.P. Mosley), pp. 399−400. New Zealand Hydrological Society, Wellington.

Smith, J.D. and McLean, S.R. (1977) Spatially-averaged flow over a wavy surface. *J. Geophys. Res.*, **82**, 1735−1746.

Soulsby, R.L., Atkins, R., Walters, C.B. and Oliver, N. (1991) Field measurements of suspended sediment over sandwaves. In: *Euromech 262—Sand Transport in Rivers, Estuaries and the Sea* (Eds R.L. Soulsby and R.E. Bettess), pp. 155−162. Balkema, Rotterdam.

Tait, S.J., Willetts, B.B. and Gallagher, M.W. (1996) The application of particle image velocimetry to the study of coherent flow structures over a stabilizing sediment bed. In: *Coherent Flow Structures in Open Channels* (Eds P.J. Ashworth, S.J. Bennett, J.L. Best and S.J. McLelland), pp. 185−201. Wiley, Chichester.

Ten Brinke, W.B.M., Wilbers, A.W.E. and Wesseling, C. (1999) Dune growth, decay and migration rates during a large-magnitude flood at a sand and mixed sand-gravel bed in the Dutch Rhine river system. In: *Fluvial Sedimentology VI* (Eds N.D. Smith and J. Rogers). *Spec. Publs Int. Ass. Sedimentol.*, **28**, 15−32.

Vendetti, J.G. and Bennett, S.J. (2000) Spectral analysis of turbulent flow and suspended sediment transport over dunes. *J. Geophys. Res.*, **105**, 22 035–22 047.

Vionnet, C., Marti, C., Amsler, M. and Rodriguez, L. (1998) The use of relative celerities of bed forms to compute sediment transport in the Paraná River. In: *Modelling Soil Erosion, Sediment Transport and Closely Related Hydrological Processes. Int. Assoc. Hydraul. Res. Spec. Publ.*, **249**, 399–406.

Villard, P.V. and Kostaschuk, R.A. (1998) The relation between shear velocity and suspended sediment concentration over dunes: Fraser Estuary, Canada. *Mar. Geol.*, **148**, 71–81.

Wewetzer, S.F.K. and Duck, R. (1999) Bedforms of the middle reaches of the Tay Estuary, Scotland. In: *Fluvial Sedimentology VI* (Eds N.D. Smith and J. Rogers). *Spec. Publs Int. Assoc. Sedimentol.*, **28**, 33–41.

Wijbenga, J.H.A. (1990) *Flow Resistance and Bed-form Dimensions for Varying Flow Conditions*. Report Q785, Delft Hydralics, Delft, 73 pp. and annexes.

Yalin, M.S. (1992) *River Mechanics.* Pergamon Press, Oxford, 219 pp.